Analysis of VFR Traffic Uncertainty and its Impact on Uncrewed Aircraft Operational Capacity at Regional Airports

Vishwanath Bulusu*, Husni Idris†, and Gano Chatterji‡
NASA Ames Research Center, Moffett Field, CA, USA

This paper proposes a method to characterize Visual Flight Rules traffic around a regional airport. The applicability of the method is discussed in the context of Uncrewed Aircraft operations at a regional airport. The relation between traffic interaction uncertainty and operational capacity at the runway is also investigated. The spatio-temporal distribution of traffic operating under Visual Flight Rules is analyzed from historical track data and visualized as heat maps generated at different altitudes. These are used to characterize the spatio-temporal uncertainty associated with traffic density, around a given airport, down to the runway. The traffic patterns at the runway are used to compute the runway capacity as a function of the probability of interaction with traffic operating under visual flight rules. Fort Worth Alliance is used as a representative regional airport for the study. Applications of the traffic characterization methods developed in this paper are also discussed.

I. Introduction

The introduction of Uncrewed Aircraft (UA) amidst conventional crewed traffic at regional airports is envisioned at scale for cargo operations [1]. The capacity to integrate this new traffic and its safety and performance will be impacted by the presence of Instrument Flight Rules (IFR) and Visual Flight Rules (VFR) traffic. Although IFR trajectories can be predicted with relatively high accuracy given their flight plans and operation under strict Air Traffic Control (ATC) supervision, VFR trajectory predictions, owing to their nature, are typically more uncertain. What is the uncertainty associated with VFR traffic and how does it impact the operational capacity for UA at a regional airport? This paper investigates these questions in terminal airspace using historical VFR track data at the regional airport.

To enable seamless integration in all airspace environments without new flight rules or segregated airspace constructs, UA are expected to be operated under today's IFR [2–4]. At commercial airports with primarily IFR traffic and minimal VFR traffic, such an integration thereby entails higher predictability for providing separation and flow management services. However, at regional airports, the proportion of VFR traffic is much higher. Since by design VFR traffic operates with minimal interaction with ATC and surveillance, the uncertainty in their location and intent is much higher. Depending on what level of VFR interaction is manageable for UA, their spatio-temporal operational capacity could be affected at regional airports. Furthermore, receiving separation services amidst this uncertainty could also lead to missed ATC communications and delays in UA maneuvering in response to controller commands, impacting flight safety [5]. It is therefore necessary to study how the operational capacity for UA is associated with different levels of VFR traffic uncertainty.

In conventional aviation, the interaction of IFR and VFR traffic is limited. Most VFR operations happen in Class G airspace entailing a natural segregation from IFR traffic. At the same time, most of the operational inefficiencies occur at major airports where big jets operate. Hence, historically, the focus has been on the operation of IFR traffic under strict ATC supervision to alleviate inefficiencies at major airports. On the other hand, pilots operating under VFR, flying in Visual Meteorological Condition (VMC), are required to see-and-avoid other traffic. As a result, there is a lack of detailed characterization of VFR traffic in aviation literature.

A few studies utilize VFR data to simulate conflicts with unmanned aircraft operations [6] or build encounter models [7]. Gariel et al. [8] made a relevant effort by analyzing six months of General Aviation (GA) traffic in the San Francisco bay terminal area. They concluded that the traffic behavior is too unpredictable. It would cause unacceptably high nuisance alarm rates on existing collision avoidance systems. They don't go further with this direction of investigation. Instead, they only use this insight as motivation for developing a novel collision alerting algorithm. UA-based cargo

*Aerospace Research Scientist, Crown Consulting Inc., Aviation Systems Division, AIAA Member
†Aerospace Research Engineer, Aviation Systems Division, AIAA Associate Fellow
‡Senior Scientist and Lead, Crown Consulting Inc., Aviation Systems Division, AIAA Associate Fellow

operations and other emerging operations such as Advanced Air Mobility (AAM) are expected to grow primarily at non-major airports, thereby increasing the frequency of interaction with VFR traffic. Characterizing the location and severity of such potential interactions could enable more informed flight planning and operations. Hence, the need to characterize VFR traffic and related uncertainty is pertinent.

To address these research needs, the authors are developing a two-step approach. The first step is to develop quantitative metrics and predictive models using historical VFR traffic data characterizing the uncertainty in a) the distribution of traffic in space and time (*spatio-temporal density*) and b) intent prediction (*intent uncertainty*) in a given region of airspace. The second step is to estimate the UA operational capacity as a function of the probability of interaction with the VFR traffic a) *analytically* and b) through fast-time simulation. This paper focuses on *characterizing the spatio-temporal density* and estimating operational capacity *analytically*. A method is presented to characterize VFR traffic in the vicinity of a regional airport by analyzing historical VFR traffic data in that airspace. The method is applied to Fort Worth Alliance (KAFW) as a representative regional airport. Heat maps, showing the distribution of traffic in a region of airspace, are developed as a means to characterize the uncertainty associated with VFR traffic density at different altitudes. VFR occupancy maps are derived from these showing the probability of VFR interaction in an airspace region. These provide further insight into runway occupancy by VFR traffic at the regional airport which is then used to derive the runway operational capacity as a function of VFR interaction uncertainty.

The rest of this paper is structured as follows. Section II describes the proposed method to characterize VFR traffic density and contextualizes it with KAFW as an example of a regional airport for such analysis. Detailed analysis results specific to the study region are presented in Section III. The flow of content in these two sections may appear repetitive. However, the difference is that the main focus of Section II is on *the method*, while the main focus of Section III is on the detailed *application of the method*. Section IV concludes the paper with a summary of the contributions and a discussion of the relevance of this work for emerging operations and directions for further exploration.

It is also noted that the operational implications of the interaction uncertainty levels are individual operator decisions that are beyond the scope of this work. The focus of this paper is only to develop a method to characterize VFR traffic density and parameterize capacity by the UA-VFR interaction uncertainty. It does not make a claim about what interaction levels are good or bad.

II. Methodology

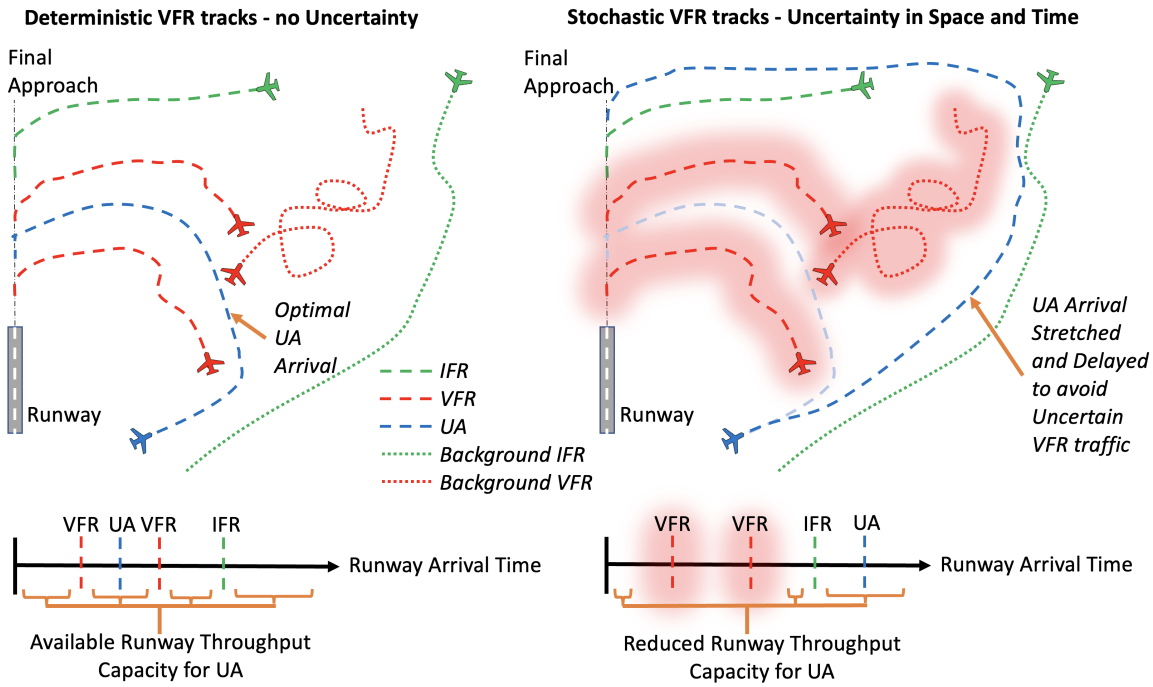

Fig. 1 Spatial and temporal impact of VFR uncertainty on UA operations

The first step is to characterize spatio-temporal density of VFR traffic around a given regional airport. Owing to strict surveillance and monitoring by multiple sources, historical IFR traffic data is highly reliable and abundant. Comparatively, historical VFR traffic data is derived primarily from pilots squawking on transponder code 1200 and surface radar detection near an airport. Hence, the data is limited and often not available for every VFR flight. Since the proportion of VFR traffic at a regional airport is relatively higher, to accommodate UA and other novel operations, it is necessary to characterize VFR behavior even with such limited data.

Fig. 1 shows an example of how stochastic VFR traffic impacts the operational capacity of a regional airport both in space and time. IFR tracks are shown in green, VFR tracks are shown in red, and UA tracks are shown in blue. Tracks into the regional airport are shown as dashed lines and background tracks are shown as dotted lines. The top row shows the spatial effects. When the IFR and VFR tracks are deterministic, separation and flow management can be more precise and would ideally require less maneuvering space. It could therefore entail a lesser workload for the controllers and the pilots. When the VFR tracks become more stochastic, for any given maneuver, the potential for UA-VFR interaction increases owing to the uncertainty in VFR position and intent. Consequently, more conservative maneuvers may be preferred to separate aircraft and manage the flows, e.g. larger path stretches and delays as illustrated in Fig. 1, thereby reducing the capacity of the terminal airspace to accommodate UA.

The bottom row in the figure shows the temporal effects. Available times with zero chance of interaction are shown in orange braces as surrogates for available runway throughput capacity for UA. When IFR and VFR traffic can be predicted precisely, more times are available to land on the runway with zero chance of interaction. Therefore more UA can be accommodated by the airport with minimal interaction with other operations. Temporal uncertainty in VFR traffic reduces the available times for UA to land with minimal chance of VFR interaction, thereby affecting the runway throughput. This paper is focused on the traffic density aspect which would capture the effects of uncertainty in the position. Intent uncertainty is being explored in parallel separately by the authors and is beyond the scope of this paper. The next section describes the case study region and the method to characterize uncertainty associated with VFR traffic density in space and time. This order of description is expected to make it easier for the reader to understand the methodology in the context of a regional airport.

A. Study Region

In this paper, KAFW is chosen as a representative regional airport. Historical traffic data for flights at KAFW was gathered for the month of September 2022. The data starts on August 31, 2022 and ends on Oct 1, 2022. The period was chosen because it had the most operations in the year in that region.

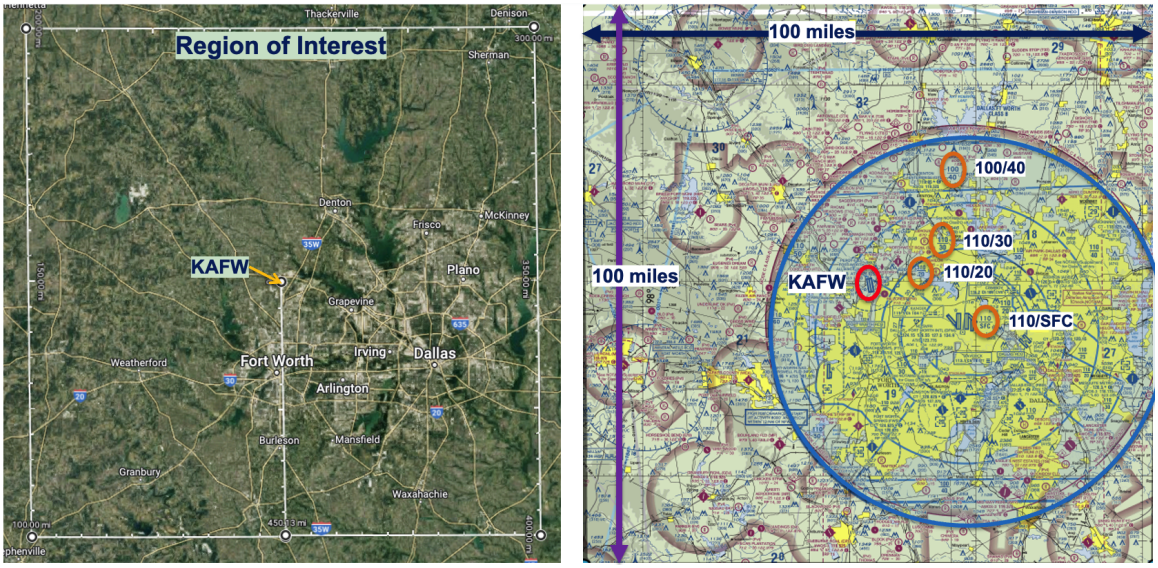

Fig. 2 Left: The region of interest (RoI) selected around KAFW demarcated by the white box (Background map credit: Imagery ©2023 Landsat/Copernicus, Imagery ©2023 TerraMetrics, Map data ©2023 Google). Right: RoI on a VFR sectional chart [9] showing controlled airspace. DFW class B airspace ceilings are highlighted.

Fig. 2 shows the selected region of interest (RoI) around KAFW. Since the goal is to characterize traffic around a regional airport, a 100 x 100-mile region is selected, centered on the regional airport (shown with a white box in the left figure). All miles mentioned in this paper are statute miles unless otherwise specified. The right figure shows a VFR sectional chart for the same RoI. VFR operations primarily use class G airspace. Operating in the vicinity of a class B, C or D airport impacts the altitudes and patterns of operation. Controlled airspace complexities are therefore important to understand to give context to VFR traffic behavior. As an example, the right figure shows the external boundaries of the Dallas-Fort Worth (KDFW) airport's class B airspace with a translucent blue circle. The inverted wedding cake structure of this class B airspace starts at different altitudes depending on the relative location from KDFW. For example, on top of KAFW, it starts at 4000 feet above Mean Sea Level (ft MSL). At the north-eastern edge of the runways, it starts at 3000 ft MSL. Roughly a couple miles southeast of KAFW it starts at 2000 ft MSL and about 6 miles southeast, it starts from the surface. KAFW itself is located at an elevation of 722 ft MSL.

Following the orientation in this figure, in the rest of this paper, all geographically oriented figures will have North pointed upwards and East to the right.

B. Spatial Density Heat Maps

To visualize and measure the distribution of VFR traffic, the RoI is divided into square grid cells of 2-mile edge length. VFR aircraft are usually responsible for visual separation with other VFR aircraft or need to maintain a lateral separation of 1.5 nautical miles (nmi) and a vertical separation of 500 feet from IFR aircraft within controlled airspace. The 2-mile grid resolution was therefore chosen after repeated trials for the best uncertainty assessment and visual characterization without making the traffic in the grid cells excessively sparse.

Fig. 3 Vertical profile of the VFR traffic data in the region of interest.

VFR traffic is restricted to fly under 18,000 ft MSL. Fig. 3 shows the vertical profile of all VFR traffic in the RoI for the month of data used. Ninety-nine percent of the traffic was under 10,000 ft MSL, 96 percent under 7000 ft MSL, 90 percent under 5600 ft MSL and 84 percent under 5000 ft MSL. The density of track points was therefore plotted over an altitude band starting from KAFW surface to 10,000 ft MSL to generate the spatial density heat map of VFR traffic in the RoI around KAFW in Fig. 4. The spatial density depicted is the number of VFR track points recorded within each cell volume for the month of data used.

The heat map in Fig. 4 shows regions of high track point density as redder and regions of low track point density as

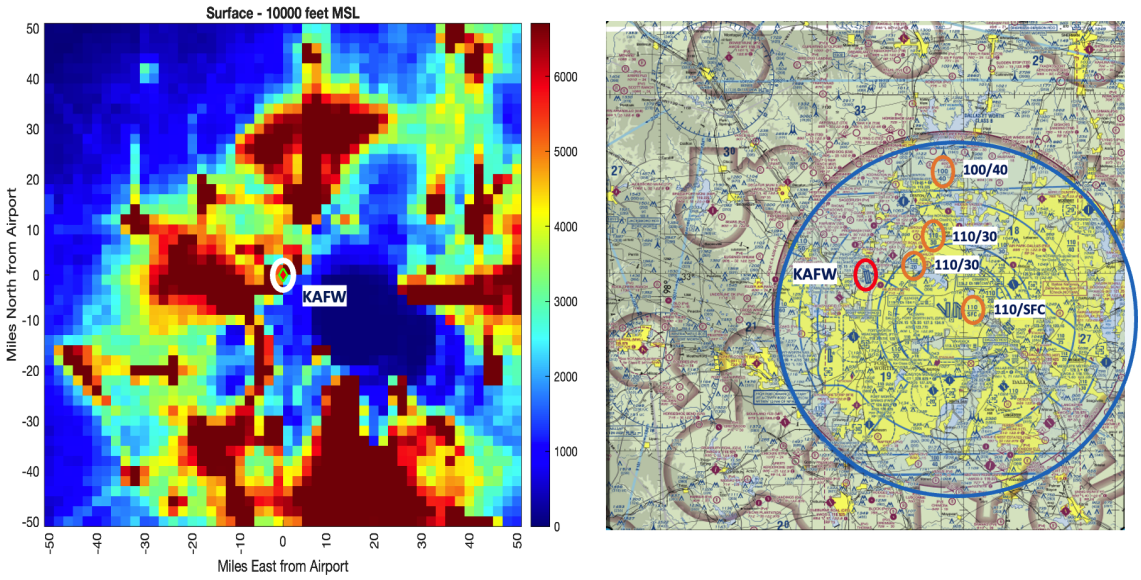

Fig. 4 Left: Spatial density heat map. Right: VFR sectional chart of RoI for reference

bluer. KAFW, in this and all further maps, is shown as a red diamond with a green outline in the center of the maps. The circular low-density blue region to the southeast of KAFW closely corresponds to the class B airspace that starts from the surface. The blue region implies that most VFR traffic in the region stays outside this airspace. Further, the redder regions in the heat map on the left correspond to the class D airports and class E airspace starting at 700 ft Above Ground Level (AGL) (shown as thick and fuzzy magenta ring-shaped features on the VFR sectional chart [9]). UA flying through redder regions would be more likely to interact with VFR traffic. To study the effect of the spatial distribution of the track data in more detail, the heatmap can be further partitioned vertically into altitude bands. The partitioning into altitude bands is presented under the results section, followed by a discussion of its use for UA flow management.

C. Spatio-temporal Occupancy Maps

Using the spatial distribution of track data, the next step is to analyze the variation of VFR traffic in the region over time. Times with higher concentrations of VFR aircraft would entail a higher probability of interaction. To measure the high VFR concentration times, a distribution of track data in time is generated over each grid cell volume, and the probability of interaction with *at least one* VFR aircraft over a given time period is calculated.

$$P\left(>1 \text{ VFR}\right) = \frac{\texttt{Number of time steps with at least 1 VFR aircraft}}{\texttt{Total number of time steps}} \tag{1}$$

Plotted over all grid cells in the RoI this generates the spatio-temporal *Occupancy Maps* of the region at different altitude bands. These are also presented under results for altitude bands up to 7000 ft MSL. The spatial aspect is captured by the location of the grid cell and the temporal aspect is captured by the probability calculation. Since each grid cell holds the temporal distribution of traffic in that cell's region, the probability of interaction with two or more VFR aircraft can also be derived by this method. Occupancy maps can also be used to study how VFR traffic interaction uncertainty varies with the day of the week or time of day. Examples of such variations are also presented in the results.

D. Runway Occupancy

Occupancy maps generated over cells in the immediate vicinity of the runway, for the surface to 2000 ft MSL altitude band, depict the runway occupancy by VFR traffic. A daily *Runway Occupancy* timeline is generated for each day in the data set. It shows at what times of the day the runways at KAFW are used by VFR aircraft. Such runway occupancy maps are useful to identify times of the day when UA can operate at the airport with minimal VFR interaction. The variation from choosing a weekday or a weekend to operate is also analyzed. To make the analysis more precise, only VFR aircraft with the first track point beginning or the last track point ending within a mile in any direction of the center of the KAFW runways were considered. The filtering is akin to producing a grid with a cell size of one mile and

selecting all the VFR traffic with their first or last track point in the four cells in the immediate vicinity of the runway center. It captured over ninety-nine percent of the VFR traffic with an estimated origin or destination airport of KAFW in the data set, while omitting all other VFR flights with neither an estimated origin or destination airport of KAFW.

E. Runway Capacity

Operational capacity can be measured in the airspace and on the runway. This paper applies its proposed method to measure runway capacity. Given the daily runway occupancy for a month, the probability of interaction with VFR traffic is calculated for every minute of the day at the runway. For a given minute (t) of the day, the probability of interaction,

$$P\left(\mathrm{t}\right) = \frac{\texttt{Number of days with VFR operation on runway during minute t}}{\texttt{Total number of days in the dataset}} \tag{2}$$

The equation is used to derive the *Runway Operational Capacity* to accommodate UA and other novel entrants. The capacity is measured in Runway Minutes as a function of the probability of interaction with VFR traffic.

Conventionally, runway capacity is measured in the number of operations per hour. However, the number of operations (arrivals and departures) would depend on the time required by each different type of aircraft. For example, assume an hour of time is available at a runway. One type of aircraft takes two minutes per operation and another type takes four minutes per operation. If the number of operations using these two aircraft types were spread out equally in the hour, on average they would take three minutes per operation. The runway operational capacity would be twenty operations per hour. If the operations used only the first type of aircraft, the runway operational capacity would be thirty operations per hour. Hence, to stay agnostic to the type of aircraft and widen the applicability of the work, the number of available *runway minutes* is chosen as a surrogate to measure runway operational capacity.

Day of week and time of day variations of VFR traffic interaction uncertainty can also be evaluated for runway capacity. Details on such variations are also discussed under results particular to the case study.

III. Results

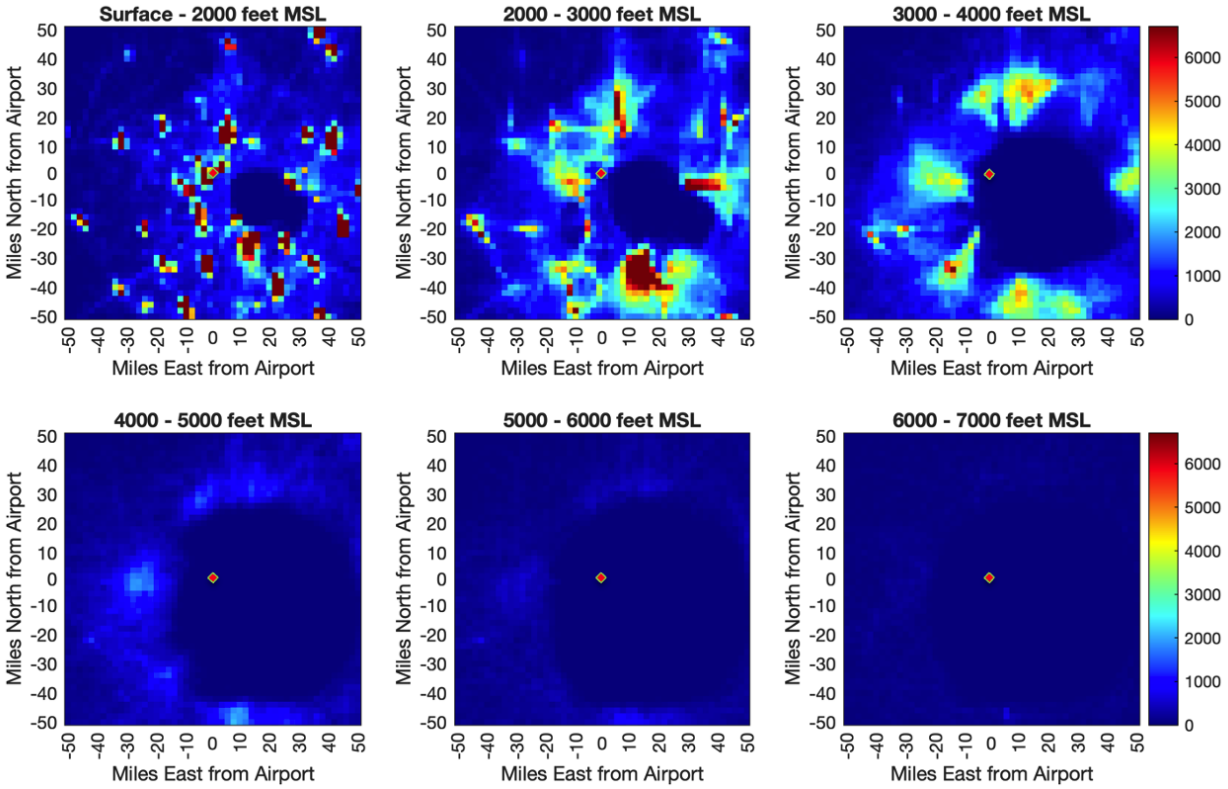

Fig. 5 Spatial density heat maps at different altitudes. Color indicates track point density.

Spatial density heat maps were generated for the KAFW RoI at different altitude bands shown in Fig. 5. Since KAFW is located at an elevation of 722 ft MSL, the first band chosen was up to 2000 ft MSL to coincide with the lowest class B ceiling in the vicinity of KAFW. Above that, bands were chosen to be 1000 ft wide to correspond with each shelf of the class B airspace. The redder regions show that more VFR track points were present in that region. These maps capture the whole month of the data used for analysis. It is noteworthy that the dark blue hole (very low to no VFR traffic) to the east of KAFW closely corresponds to the KDFW class B and grows in size with altitude.

These maps bring out three types of insights. First, the redder and brighter regions coincide with the locations of the regional airports in the area such as Denton Enterprise (KDTO) to the north of KAFW and Forth Worth Meacham (KFTW) to the south. Hence, VFR traffic in the region is concentrated at or around these airports. Second, the majority of the traffic was present between 2000 ft to 4000 ft MSL altitudes and spread across a wider portion of the RoI as shown by huge swaths of yellow and red. This distribution is likely caused by the inverted wedding cake structure of the Dallas-Forth Worth class B airspace. Third, above 3000 ft MSL, there are natural channeled gaps between VFR-heavy regions that could be potentially utilized by UA and other novel entrants. Such utilization is useful for strategic flight planning and flow management decisions. The extent to which these gaps can be utilized would also depend on the UA performance characteristics, arrival/departure route geometry, and altitude constraints along the route.

Under 3000 ft MSL, VFR traffic is concentrated roughly similarly at both north and south approaches to KAFW. Approaches to integrating UA within the traffic pattern at the airport would therefore be helpful at these altitudes. These approaches could be individually tailored to a given regional airport, automated, and implemented on UA.

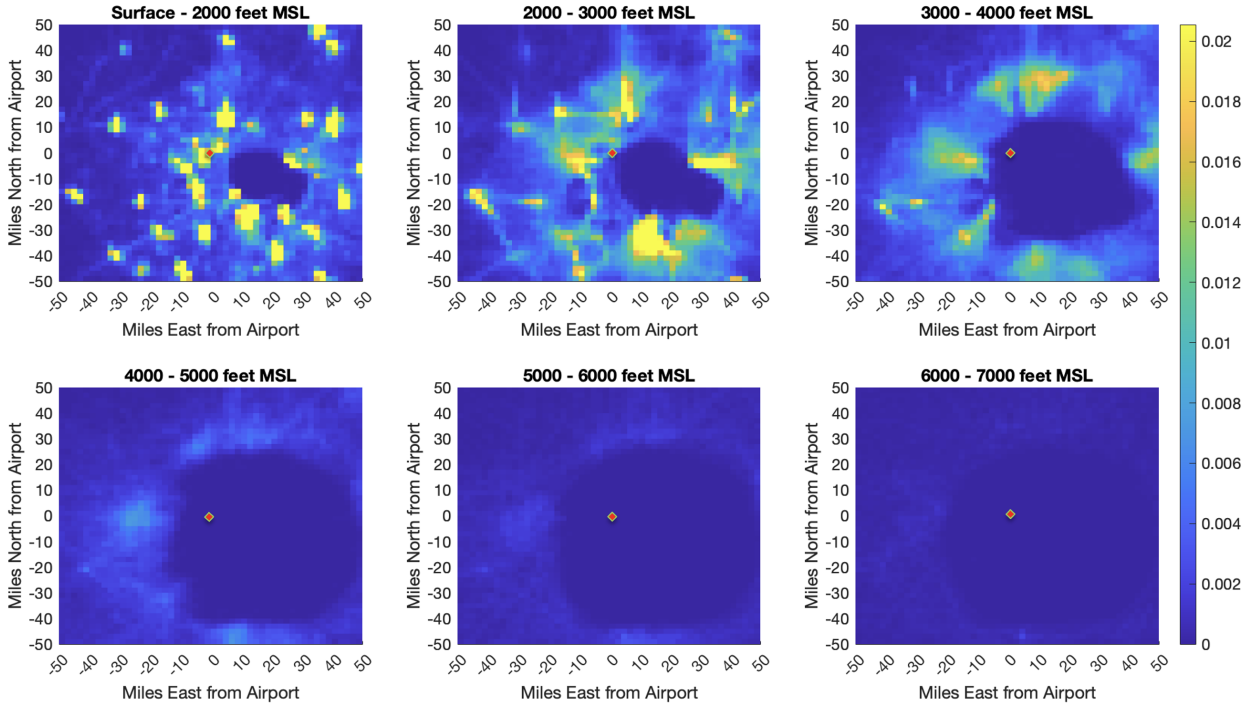

Fig. 6 Spatio-temporal occupancy maps at different altitudes. Color indicates the probability of interaction.

Using the heatmaps, occupancy maps were generated at the same altitude bands to measure the probability of interaction with VFR traffic. These are shown in Fig 6. In addition to providing similar spatial information as the heat maps, these quantify the temporal uncertainty of interacting with VFR traffic in regions of high traffic density. For example, between the 3000-4000 ft MSL band, the highest interaction probability observed was 0.02 compared to around 0.24 under 2000 ft MSL. That entails an order of growth in the risk of interaction. The risk of interacting with VFR traffic is negligible above 4000 ft MSL. Therefore, the remaining results presented for occupancy maps will consolidate the data from the surface to 4000 ft MSL. This is done for brevity in presenting other example applications of occupancy maps.

As noted earlier, the probability of interaction with at least two VFR aircraft, at least three VFR aircraft, and so on, within each cell, can also be computed by using this method, in general. In particular to the case study in this paper,

given the chosen grid cell size of 2 miles, very rarely are there more than two VFR aircraft within the same grid cell at the same time. Hence, the probability of interaction with at least two (or more) VFR aircraft within a grid cell would diminish rapidly and is therefore not shown. However, it is also noted that one could still interact with two or more VFR aircraft over multiple cells. The probability of such interaction can therefore be re-computed jointly over the cells traversed by the UA's route.

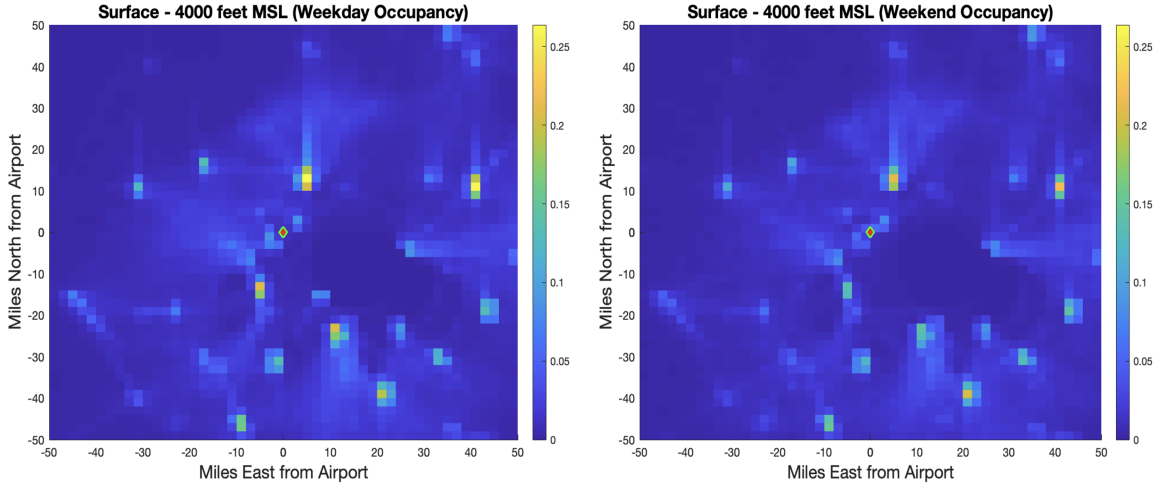

Fig. 7 Comparison of occupancy maps on weekday and weekend. Color indicates the probability of interaction.

Occupancy maps can also be used to study variations in traffic densities based on the day of the week and the time of the day. For example, Fig. 7 compares the occupancy maps for a weekday with that produced for a weekend. Although the spatial effect is similar, the probability of interaction is reduced by around five percent during weekends.

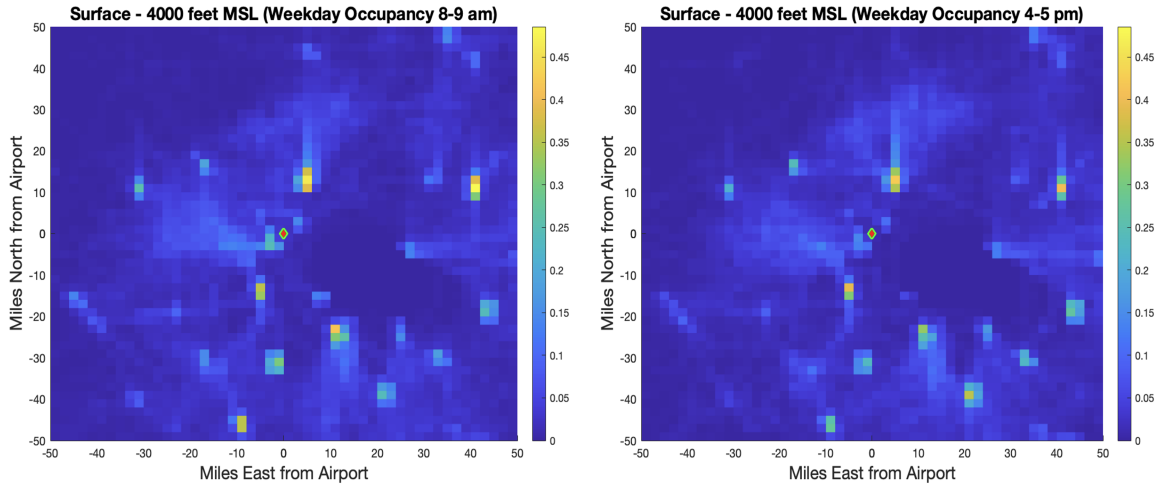

Fig. 8 Comparison of occupancy maps at different times of the day. Color indicates the probability of interaction.

Even for a given weekday, the time of day had a more pronounced effect. For example, Fig. 8 compares the occupancy map for weekday traffic between 8 am to 9 am with that for weekday traffic between 4 pm to 5 pm. Here, flying in the evening could reduce the probability of VFR interaction in the immediate vicinity of KAFW from around 0.3 to about 0.15, reducing the chance of encountering a VFR aircraft by half. The risk associated with a given probability of interaction is a matter of operator preference. Qualifying how much risk is good or bad is beyond the scope of this paper.

Overall, the occupancy maps provide another useful input for UA scheduling and strategic de-confliction. Occupancy maps for different times of day, if continuously updated with the most recent VFR traffic data in the region, could also help de-confliction over shorter time horizons.

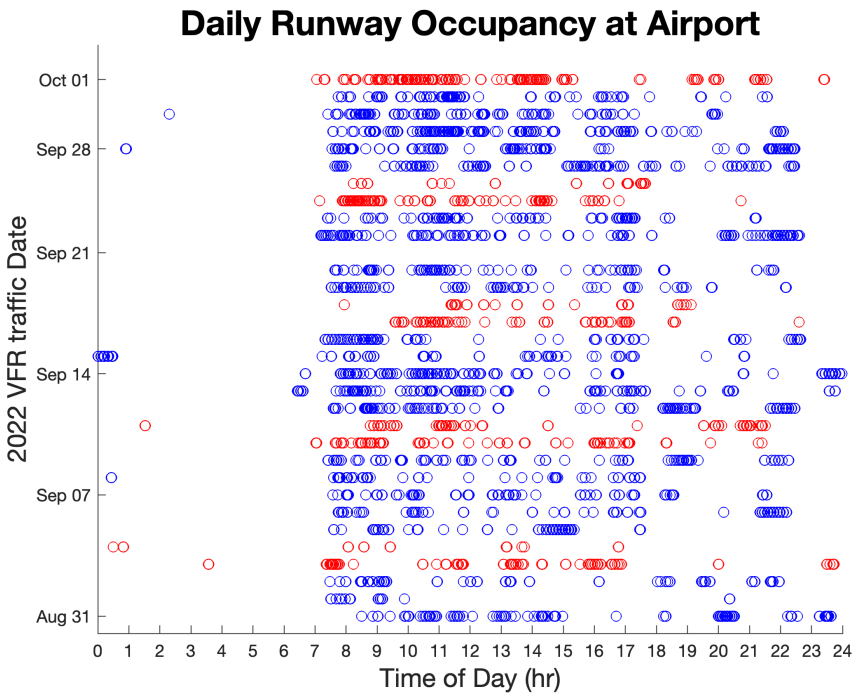

Fig. 9 Runway occupancy variation for all days of data. Weekdays - Blue, Weekends - Red.

Each grid cell stores the time history of VFR track data traversing its region over a given period. At the surface, the grid cell directly over the runway characterizes the runway occupancy by VFR traffic. Fig. 9 shows the runway occupancy plotted for each day in the data set. Each marker represents a minute of the day during which a VFR aircraft landed at the runway. The detailed breakdown of a day provides insight into when there are windows for UA operation with minimal VFR interaction. For example, on August 31, no VFR operated at KAFW before 8:20 am; a few minutes were available between noon to 1 pm that had no VFR occupying the runway; between 5 pm to 8 pm, VFR aircraft occupied the runway for only 5 minutes, and so on.

Weekdays are shown as blue circles and weekends are shown as red circles. Overall, VFR operations at KAFW peak between morning 7 am to evening 5 pm. On weekdays, the spread between these hours is very even, while on weekends, the major peaks happen during the earlier hours of the day. Before 7 am, there is minimal VFR traffic. Late hours (5 pm - midnight), although not as sparse, also have several time periods with minimal VFR interaction. It could be useful for planning batch cargo operations if UA are equipped to operate at early and late hours.

Fig. 10 shows the probability of interaction at the runway derived from the runway occupancy data. The top row shows the probability with all days equally weighted. The second row shows the distribution, given the day of interest is a weekday. The third row repeats this for a weekend. As stated earlier, this is another way of depicting that the operations on weekdays are more evenly spread out while on weekends there are several gaps in the day where UA could operate with no VFR interaction. Graphs like these could be useful for both strategic planning of operations and tactical decision-making during the day. For example, during an on-demand operation, where a UA must take off or land within a specific time window, this provides a way to quantify the chance of encountering VFR traffic. A UA operator could use that information to delay, hasten or leave an operation unchanged, based on the level of risk the operator is willing to undertake.

The runway occupancy analysis can next be used to measure the runway operational capacity for UA with regard to VFR interaction. Figure 11 shows this with the translucent bars. It captures the operational capacity of the runway as a resource, measured in runway minutes parameterized by the probability of VFR interaction. Again, the weekday and weekend effects are separated for comparison. Close to 300 minutes of additional time was available on weekends with no chance of VFR interaction, while an additional 500 minutes of low-chance (under 10 percent) minutes were available on weekdays compared to weekends that had no minutes available with under 10 percent chance of interaction. The distribution of these minutes during the day was already captured by the previous interaction and occupancy figures.

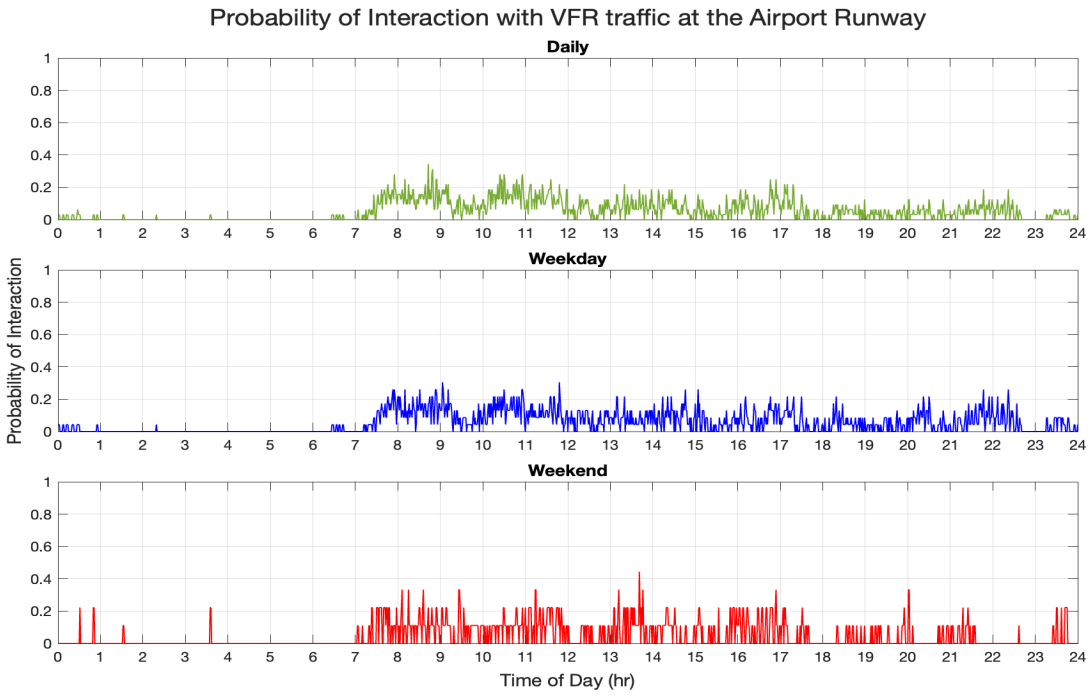

Fig. 10 Probability of interaction with VFR traffic over 24 hours and comparison with weekdays and weekends.

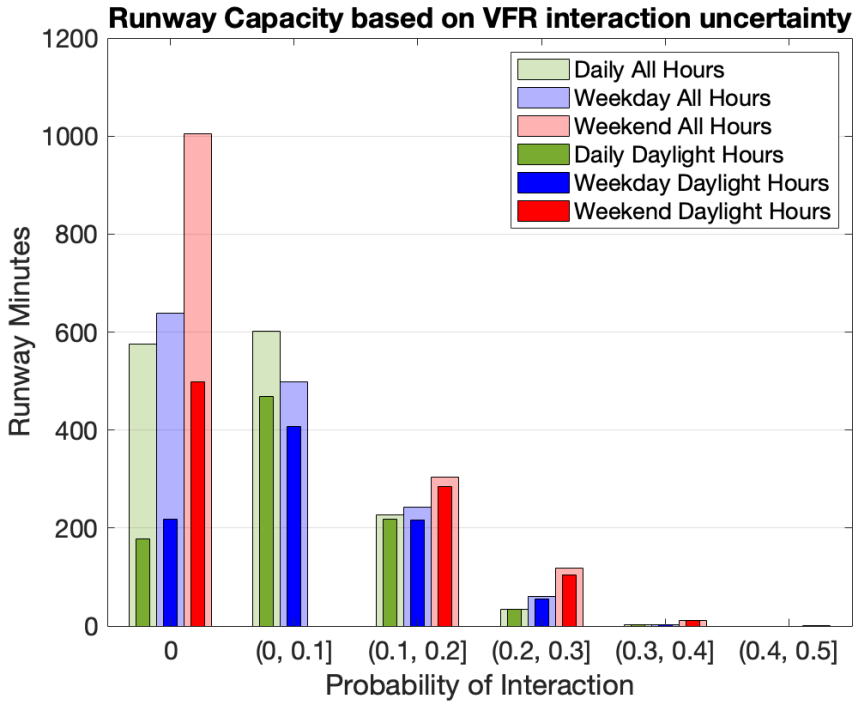

Fig. 11 Runway capacity measured in runway minutes available as a function of the probability of interaction with VFR traffic

It is also quite possible that a UA operator might prefer to operate only during daylight hours for example due to on-board sensor visibility limitations. Hence, the runway occupancy analysis is repeated for daylight hours. In the chosen study region, during September, there is sufficient daylight for visibility considerations from approximately 6 am to 9 pm. Hence, the runway minutes are also characterized only for these daylight hours. The opaque bars in Fig. 11 show their distribution. Over half of the minutes with no chance of VFR interaction were during non-daylight hours. Yet close to 200 such minutes are still available on any given day. If a chosen day is a weekend, there are additional 280 such minutes available compared to weekdays. Minutes available with under 10 percent chance of interaction are only reduced by about one-tenth. Finally, minutes with a higher chance of interaction are minimally affected as they occur primarily during daylight hours.

IV. Conclusion

This paper presented a method to characterize the uncertainty associated with VFR traffic spatial and temporal density in the vicinity of a regional airport. This analysis was then applied to measure the impact on UA operational capacity at the regional airport. Historical VFR traffic was used to generate spatial density heatmaps around a regional airport at different altitude bands. These were used to develop spatio-temporal occupancy maps that capture the probability of interacting with VFR traffic at a given place and time. The same information was generated at the runway to produce runway occupancy maps. These maps were used to characterize the interaction probability with VFR traffic at different times of the day. This in turn captured the runway capacity in minutes available to accommodate UA traffic as a function of VFR interaction uncertainty.

As an example case study, this method was applied to KAFW regional airport and a month of VFR traffic data was characterized. Occupancy maps showed promise in additionally capturing the day of the week and time of day effects, which may be useful for strategic and tactical flow management decision-making. This research fills an important gap of the lack of detailed VFR traffic characterization in aviation literature. As stated earlier, this paper is the first step towards bridging that gap. Future work will characterize the uncertainty in intent and then derive capacity measures with associated safety and performance metrics through fast-time simulation. Eventually, these methods can be released as a toolkit that would be equally useful for autonomous cargo and the broader AAM industry.

Acknowledgments

This work is funded by NASA's Pathfinding for Airspace with Autonomous Vehicles sub-project.

References

[1] Hayashi, M., Idris, H., Sakakeeny, J., and Jack, D., "PAAV Concept Document," 2022.

[2] Gigarjill, M., "Integration of Unmanned Aircraft Systems into the National Airspace System Concept of Operations," *Federal Aviation Administration*, 2012, pp. 1–120.

[3] SC-228, R. F., *Minimum Operational Performance Standards (MOPS) for Detect and Avoid (DAA) Systems*, RTCA, Incorporated, 2017.

[4] Johnson, W. C., and Shively, R. J., "UAS Detect and Avoid: Efforts from NASA's UAS Integration into the NAS Project," *2018 Aviation Technology, Integration, and Operations Conference*, 2018, p. 2871.

[5] Bulusu, V., Chatterji, G. B., Lauderdale, T. A., Sakakeeny, J., and Idris, H. R., "Impact of Latency and Reliability on Separation Assurance with Remotely Piloted Aircraft in Terminal Operations," *AIAA AVIATION 2022 Forum*, 2022, p. 3704.

[6] Johnson, M., Santiago, C., and Mueller, E., "Characteristics of a well clear definition and alerting criteria for encounters between uas and manned aircraft in class e airspace," *Air Traffic Management (ATM) Research and Development Seminar*, 2015.

[7] Adaska, J. W., "Computing risk for unmanned aircraft self separation with maneuvering intruders," *2012 IEEE/AIAA 31st Digital Avionics Systems Conference (DASC)*, IEEE, 2012, pp. 8A4–1.

[8] Gariel, M., Hansman, R. J., and Frazzoli, E., "Impact of GPS and ADS-B reported accuracy on conflict detection performance in dense traffic," *11th AIAA Aviation Technology, Integration, and Operations (ATIO) Conference, including the AIAA Balloon Systems Conference and 19th AIAA Lighter-Than*, 2011, p. 6893.

[9] "FAA Sectional Chart for Dallas-Fort Worth Area," `https://www.faa.gov/air_traffic/flight_info/aeronav/productcatalog/VFRCharts/Sectional/`, 2023. Images produced by the U.S. Government and in the public domain.